A New mmWave Rectangular Microstrip Patch Antenna for Breast Tumor Detection

Shamiul Ashraf Shoishob and Mostafa Zaman Chowdhury

February 19, 2024

A New mmWave Rectangular Microstrip Patch Antenna for Breast Tumor Detection

******* ****** ********** ******* ***** *********** ******* *******
*****
*********** ** ********** *** ********** ************ ****** ********** ** *********** *
*********** ************ *********
*********** ** *********** ************ ******* *********** ************ ***** *****

ABSTRACT- An inset feed microstrip patch antenna created for biological purposes is presented in this paper. The feed line length and radiating patch width were increased to their full potential, which boosted the antenna's performance. The antenna is 4.7x4.7x0.508 mm3 and operates in the Q band, also known as the Scientific and Medical (ISM) band. At 1.19 GHz, the antenna exhibits excellent efficiency with a 91.65% bandwidth. The antenna has a three-layer breast phantom incorporated into it, and other performance factors, such as the electric field intensity and reflection coefficient, are affected by the presence of a tumor. It is possible to pinpoint the tumor's position and size by keeping an eye on changes in the antenna's return loss and transmission coefficient.

Index Terms- Breast-tumor, mmWave imaging, Radiation efficiency, SAR, S-parameters, Return loss, Transmission co-efficient.

I. INTRODUCTION

On-body communication frequency ranges are recommended by the IEEE 802.15.6, and microstrip antennas are the favored option because to their low cost and ease of production [7-8]. The antennas used for on-body communication must be flexible, robust, and offer a dependable communication link while complying with the rules for human safety set out by the Federal Communications Commission. The specific absorption rate (SAR), which measures how much electromagnetic radiation the human body absorbs, can influence antenna performance characteristics when radiating objects are placed close to people. According to FCC standards, the sustainable value of SAR for the head and body is 0.90 W/Kg and 1.25 W/Kg, respectively [5]. A ground radiating on-body antenna, a monopole on-body antenna, a bowtie antenna, and a microstrip antenna are among the other on-body antennas.

II. DESIGN OF THE MICROSTRIP ANTENNA

The patch element of a rectangular patch antenna using a perfect electric conductor (PEC) is discussed in the chapter. It is printed on a lossy substrate with a dielectric constant of 2.2 and has a thickness of 0.508 mm. 33 GHz is the antenna's operating frequency.

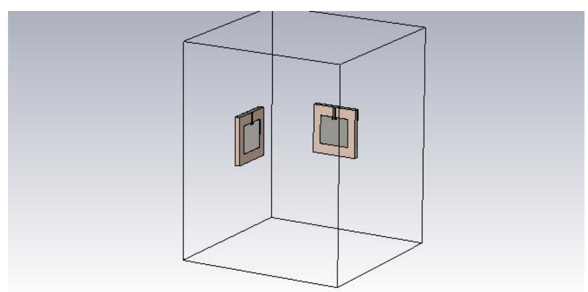

Figure 1: Designed of the proposed micro-strip patch antenna.

Figure 1 depicts the suggested antenna, and two more antennas of a similar design have been created. The antenna's modest substrate dimensions are 4.7 mm in length and breadth, and all conceivable graphs are taken between 30 and 40 GHz. The antennae are spaced 8.48 mm apart, however this spacing may be altered to identify tumors larger than that.

The patch length and patch width, as well as the substrate height, which is only around 0.508 mm, are all listed in Table 1.

Table 1: Parameter list of the proposed microstrip patch antenna

Parameters	Value
Substrate Length, SL	4.7 mm
Substrate Width, SW	4.7 mm
Substrate Height, SH	0.508 mm
Patch Length, PL	2.75 mm
Patch Width, PW	3.1 mm
Height of Conductor, Mt	0.035 mm
Gap between patch and feed, MW	0.2 mm
Inset Length, inL	0.2 mm
Inset Width, inW	0.15 mm
Distance between two antenna, d	8.48 mm
Design Frequency, f	33 GHz

III. DESIGN SOFTWARE

The suggested antenna design was developed using the 3-dimensional electromagnetic analysis program CST (Computer Simulation Technology) STUDIO 2019, according to the passage. The program enables the design, investigation, and improvement of electromagnetic components and systems. The user-friendly interface of CST Studio Suite provides a variety of electromagnetic technologies for activities across the electromagnetic spectrum.

IV. DESIGN OF THE PHANTOM MODEL

We may infer from the text that the study's phantom model contains three layers: breast skin, breast fat, and fibro-glandular tissue. The permittivity and tangent loss values differ for each layer. The performance of the antenna will be impacted by the tumor inside the phantom model, which has a greater tangent loss value. Table 2 lists the permittivity and tangent loss values for each layer and the tumor at 33 GHz.

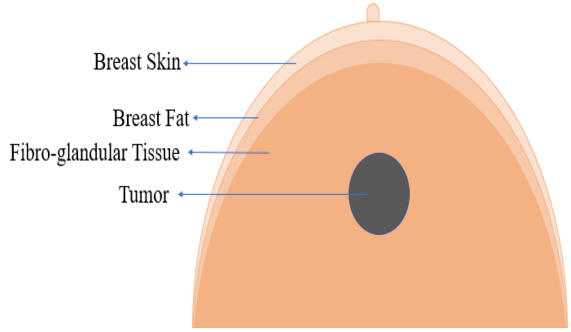

Figure 2: Design view of breast phantom model.

Figure 2 displays the suggested model's design picture, which was generated using CST Studio Suite 2019. Permittivity and tangent loss input parameters for each layer and tumor were correctly taken into consideration. At various frequencies, these values may be calculated analytically or empirically; in this study, 33 GHz was employed [9-11].

Table 2: loss tangent and permittivity values for breast three layers and tumor cell

f GHz	Tissues	Permittivity (ε_r)	Tangent loss ($\tan\delta$)
33	Skin	17.7	0.93
33	Fat	3.4	0.16
33	Fibro-glandular	16	0.94
33	Tumor	18	1.05

Figure 3 shows the simulated design image of this thesis. All the specific parameters with correct values are input perfectly. The values of permittivity and tangent loss for different frequency for all the three-layers and tumor cell can be calculated mathematically or experimentally. For the applications of high frequency, here 33 GHz frequency is used.

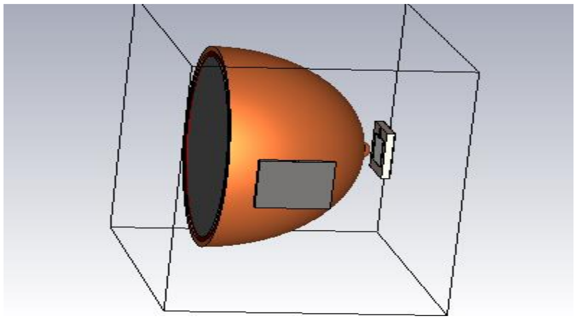

Figure 3: Breast phantom model with two antennas.

V. SIMULATED RESULTS AND DISCUSSIONS

A. RETURN LOSS(S1,1)

At the very first, we are going to see return loss of two antenna having no tumor cell. The $S_{1,1}$ value at 33 GHz frequency is about -9.6528 dB in Figure 4. And the lowest value is about -11.2 dB at 32.2 GHz frequency.

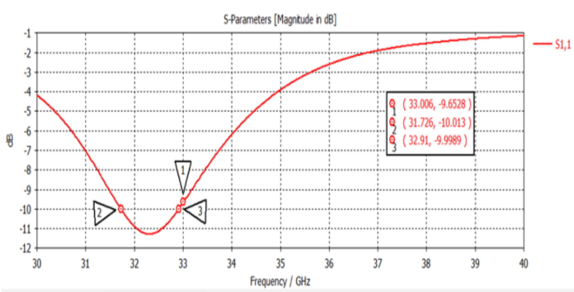

Figure 4: $S_{1,1}$ or return loss while using only two Antenna.

The performance of the antenna with various tumor cell sizes is shown in Figure 5. The measurement performed has a bandwidth of 14100 MHz and is called the reflection coefficient $S_{1,1}$. Tumor cells with diameters of 0.9 mm, 1.5 mm, and 3 mm have return loss values of -7.897 dB, -7.853 dB, and -7.649 dB at 33 GHz, respectively. The return loss graph, however, is unable to effectively distinguish between the various tumor sizes on its own.

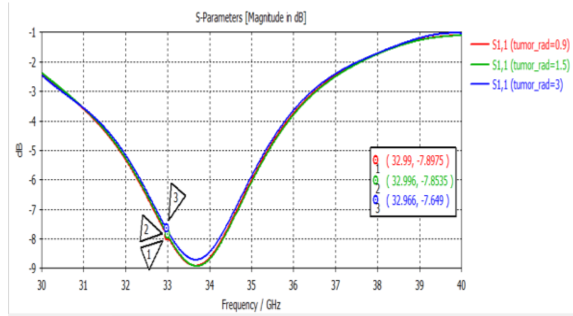

Figure 5: $S_{1,1}$ or return loss for different sized tumor cell.

The value of 3 mm sized tumor cell is less in magnitude than 0 mm sized tumor cell. For the negative sign it is clear that return loss of cell having tumor is bigger than fresh human phantom model. One thing is clear that the value of $S_{2,2}$ will be almost similar with $S_{1,1}$. So, no need to plot the graph of $S_{2,2}$.

B. TRANSMISSION CO-EFFICIENT($S_{2,1}$) PERFORMANCE.

We will see the value of $S_{2,1}$ at resonant frequency of different sized tumor cell in Figure 6. The value of $S_{2,1}$ of 0.9 mm, 1.5 mm sized tumor cell is -60.648. These two values are similar. The value of $S_{2,1}$ of 3 mm sized tumor cell is -64.402 dB. The resonant frequency is 34.599 GHz for 0.9 mm and 1.5 mm sized tumor and 38.84 GHz for 3 mm sized tumor cell. So, frequency will be more distorted for higher tumor cell.

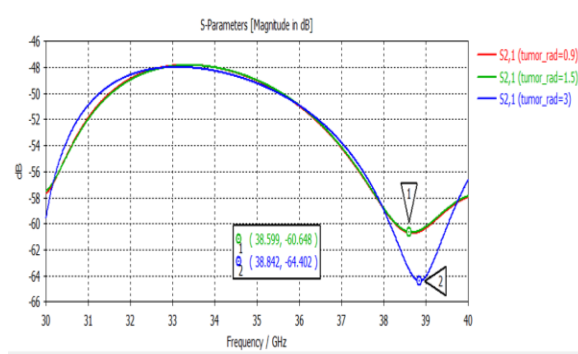

Figure 6: $S_{2,1}$ or transmission co-efficient for different sized tumor cell.

Here, by analyzing the graph transmission co-efficient for no tumor cell will most. And transmission co-efficient for highest tumor cell size will be least. It is the value when antenna-1 is excited and backscattered signals from antenna-1 are received by antenna-2. With the aid of resonant frequency, we can differentiate the tumor size between 3 mm and 1.5 mm.

C. EXISTENCE OF TUMOR CELL BY PORT SIGNALS

The following Figure 7(a) and 8(b) will detect the existence of tumor cell in the phantom model. We can see from these two graph, the peak value of the fresh phantom model is 0.15 W^(1/2) before 5 ns. And the peak value for all the tumor cell is 0.003 W^(1/2) after 5 ns. So, it is almost 50 times less than the freshy one. It is clearly describe, any antenna facing any kind of obstacles will give less value of port signals.

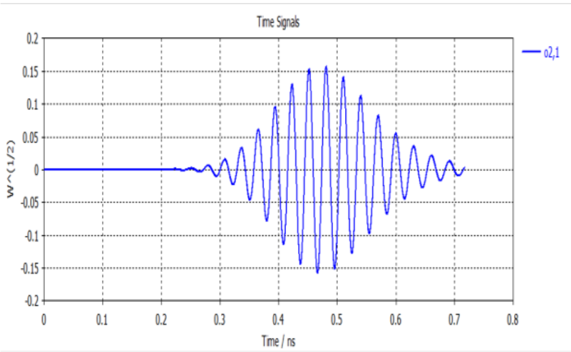

(a)

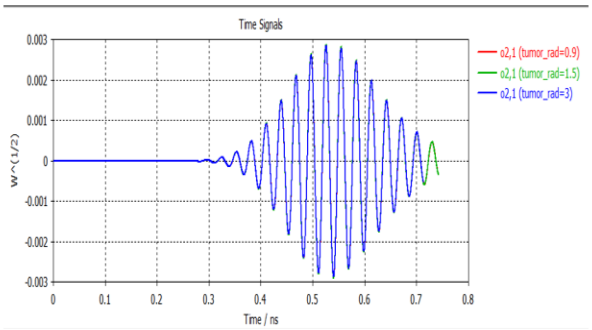

(b)

Figure 7: Simulated port signals value of phantom model, (a) having no tumor cell, (b) having different sized tumor cell.

D. SPECIFIC ABSORBTION RATIO (SAR)

The SAR value determination is important for the purpose of patient safety. According to ICNRP practical value of SAR which is not harmful to human tissue is 0.467 W/kg. The proposed antenna gives SAR value of 0.445 W/kg which is safe in the following Figure 8.

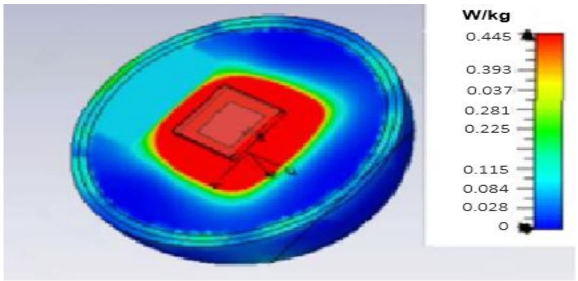

Figure 8: Simulated SAR analysis of phantom model with tumor cell.

E. TUMOR CELL LOCALIZATION

For tumor cell localization, we were using 3 co-ordinate parameters. These are Tx, Ty and Tz in the direction of x, y and z axis. Different values of Tx, Ty and Tz gives the different position in the tumor in the phantom model. We can modify Tx, Ty and Tz from the values 0 to 4 in this directional axis in my thesis. As a result, possible no. of 96 integer position can have for the tumor cell. Figure 9 will describe the tumor cell localization.

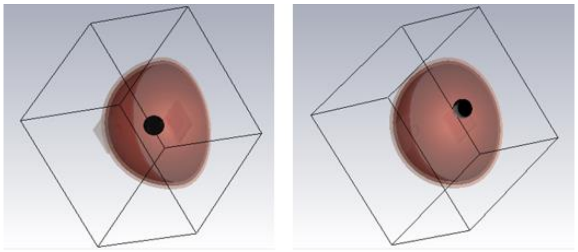

(a) (b)

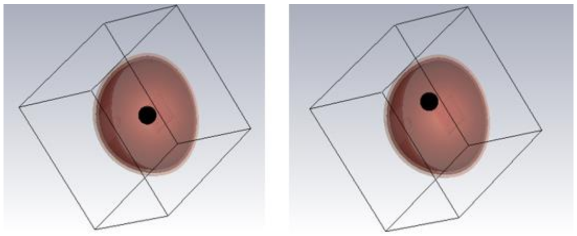

(c) (d)

Figure 9: Different tumor location of 1.5 mm tumor cell by assuming, a) (Tx Ty Tz) = (0 0 4) b) (Tx Ty Tz) = (1 2 0) c) (Tx Ty Tz) = (1 0 2) d) (Tx Ty Tz) = (4 0 0).

Thus, different axis value changes the tumor position. And the different tumor position will have different electric field, magnetic field, VSWR, Scattering parameters values.

VI. COMPARISON

By demonstrating in Table 3, the suggested antenna resolves the shortcomings of earlier research. It can detect the smallest tumor size of 1.5 mm, has a modest dimension that lowers design costs, and is efficient for early-stage tumor detection. The proposed antenna significantly outperforms earlier work with the maximum efficiency of 91.65% among all the reference.

Table 3: Comparison between antenna in paper works and proposed antenna

Reference	Dimension (mm^3)	Tumor Size (mm)	Frequency (GHz)	Gain (dB)	Efficiency (%)	Imaging	Application
[1]	88.00× 75.00× 1.6	10	1.54	8.50	91.20	Back Scattered Signal Imaging Algorithm	Microwave Breast Imaging
[2]	54.24× 54.24× 1.0	5	0 to 10	4.23	58.30	Scattering parameters	mmWave Breast Imaging
[3]	30.00× 25.00× 1.6	>10	2.7 to 10.3	5.81	81.70	Scattering parameters	Microwave Breast Imaging
[4]	5.00× 5.00× 0.578	2	30 to 40	6.65	91.46	Scattering parameters , IC-DAS and SAR Analysis	mmWave Breast Imaging and 5G
[6]	40.00× 40.00× 1.6	10	3.01 to 11	7.1	91.30	DMAS algorithm	Microwave Breast Imaging
This Paper	**4.70× 4.70× 0.508**	**1.5 to 3**	30 to 40	6.18	**91.65**	Scattering parameters (S_{11} to S_{22}),	mmWave Breast Imaging

VII. CONCLUSION

The suggested antenna is appropriate for on-body biomedical applications because to its large bandwidth and efficiency of 91.65%. With just two antennas, its directivity of 6.743 dB enables high-performance output. With a high frequency of 33 GHz, the antenna can locate tumor cells anywhere in the human phantom model that are 1.5 to 3 mm in diameter. The antenna is helpful for microwave imaging and can be utilized in Q band communications.

VIII. REFERENCES

[1]. M. T. Islam, M. Z. Mahmud, N. Misran, J. -I. Takada, and M. Cho, “Microwave Breast Phantom Measurement System with Compact Side Slotted Directional Antenna,” *IEEE Access*, vol. 5, pp. 5321-5330, 2017.

[2]. A. Aziz, D. Ahmad, T. A. Shila, S. Rana, R. R. Hasan, and M. A. Rahman, “On-Body Circular Patch Antenna for Breast Cancer Detection,” *IEEE International Electromagnetics and Antenna Conference (IEMANTENNA)*, vol. 2, pp. 029-034, 2019.

[3]. F. M. Eltigani, M. A. A. Yahya, and M. E. Osman, “Microwave Imaging System for Early Detection of Breast Cancer,” *International Conference on Communication, Control, Computing and Electronics Engineering (ICCCCEE)*, pp. 1-5, 2017.

[4]. C. Das, M. Z. Chowdhury, and Y. M. Jang, “A Novel Miniaturized mmWave Antenna Sensor for Breast Tumor Detection and 5G Communication,” *IEEE Access*, vol. 10, pp. 114856-114868, 2022.

[5]. R. S. Kshetrimayum, “Mobile Phones: Bad for Your Health,” *IEEE Potentials*, vol. 27, no. 2, pp. 18-20, 2008.

[6]. M.T. Islam, M. Samsuzzaman, S. Kibria, and M. J. Singh, “A Homogeneous Breast Phantom Measurement System with an Improved Modified Microwave Imaging Antenna Sensor,” *Annual Review of Biomedical Engineering*, pp. 274-290, 2018.

[7]. S. Sukhija, and R. K. Sarin, “Design and Performance of Two-sleeve Low Profile Antenna for Bio-medical Applications,” *Journal of Electrical Systems and Information Technology*, vol. 4, pp. 49-61, 2017.

[8]. Y. Hao, A. Alomainy, P. S. Hall, Y. I. Nechayev, C. G. Parini and C. C. Constantinou, “Antennas and propagation for body centric wireless communications,” *International Conference on Wireless Communications and Applied Computational Electromagnetics*, pp. 586-589, 2005.

[9]. B. S. Abirami, and E. F. Sundarsingh, “EBG-Backed Flexible Printed Yagi–Uda Antenna for On-Body Communication,” *IEEE Transactions on Antennas and Propagation*, vol. 65, no. 7, pp. 3762-3765, July 2017.

[10]. V. Selvaraj, P. Srinivasan, J. Kumar, R. Krishnan, and K. Annamalai, “Highly Directional Microstrip Ultrawide Band Antenna for Microwave Imaging System,” *Acta Graphica*, vol. 28, no. 1, pp. 35–40, 2017.

[11]. E. C. Fear, J. Bourqui, C. Curtis, D. Mew, B. Docktor, and C. Romano, “Microwave Breast Imaging with A Monostatic Radar Based System: A Study of Application to Patients,” *IEEE Trans. Microw. Theory Tech.*, vol. 61, no. 5, pp. 2119–2128, May 2013.